Hindawi
Journal of Sensors
Volume 2020, Article ID 1237469, 13 pages
https://doi.org/10.1155/2020/1237469

Research Article

Study on Energy Acquisition Scheme and Parameter Optimization for Double-Insulated Ground Wire of Overhead Transmission Lines

Lifu He,[1,2] **Bo Li**,[1,2] **Guoyong Zhang**,[1,2] **Xiudong Zhou**,[1,2] **and Jing Luo**[1,2]

[1]*State Key Laboratory of Disaster Prevention and Reduction for Power Grid Transmission and Distribution Equipment, Changsha 410129, China*
[2]*State Grid Hunan Electric Company Limited Disaster Prevention and Reduction Center, Changsha 410129, China*

Correspondence should be addressed to Lifu He; 837684304@qq.com

Received 20 December 2019; Revised 14 May 2020; Accepted 25 May 2020; Published 19 June 2020

Academic Editor: Antonio Lazaro

An energy acquisition system for the ground wire of an overhead transmission line can provide a continuous and stable power supply for an on-line monitoring device. Its key issue is how to obtain enough power. To solve this problem, an energy acquisition scheme based on the double-insulated ground wire of an overhead transmission line has been investigated in this study. Three energy acquisition schemes were proposed, equivalent circuit analysis models of the three energy acquisition schemes were established, and the maximum power acquired was theoretically analyzed. The energy acquisition power of the three energy acquisition schemes for different tower-type sizes was also analyzed. A simulation model was built in PSCAD. The effects of load impedance, length of energy acquisition wire, grounding resistance, and load current on the power acquired were analyzed. The research results of this paper provide theoretical guidance for choosing an energy acquisition scheme and for designing key parameters in practice.

1. Introduction

With the increasing dependence of society on electric energy, the reliability requirements of stable power grid operation are becoming ever more demanding, and hence, a large number of on-line monitoring devices have been put into operation on transmission lines. Due to the lack of a continuous and stable low-voltage power supply, on-line transmission line monitoring devices are usually powered by solar cells, small wind turbines, and batteries. The stability of this power supply is greatly affected by the weather, and the output power is small, the volume of the device is large, and the economy is poor. The need for a power supply with sufficient power and continuous stability has become the development bottleneck of on-line transmission line monitoring devices. According to the principle of electromagnetic induction, there is induction voltage on the overhead ground wire [1], and a current loop can be formed between the two ground wires or between the ground wire and the earth [2]. According to relevant research estimates, the circulation energy loss between the overhead ground lines of a common 220 kV transmission line is 34138 kWh per year [3]. Hence, an energy acquisition technology using the overhead ground wire can provide sustainable and stable electric energy and is the most promising means to solve the power supply problem for on-line transmission line monitoring devices. However, at present, only a small amount of power can be taken from the ground wire, and a method to obtain sufficient power from the ground line to meet the power demand of the on-line monitoring device has not yet been developed. Therefore, it is of great practical value to study ground wire energy acquisition technology.

At present, some researchers have carried out studies on energy acquisition technology for overhead transmission lines. References [4–8] investigated energy acquisition technology for high-voltage transmission lines. However, a high-potential energy acquisition system cannot supply power to a ground potential monitoring device. References

[9, 10] proposed a method of extracting energy from overhead high-voltage power lines and transmitting it from the power line to a monitoring device on a tower through wireless transmission in a magnetically coupled resonant configuration. Reference [11] proposed an integrated capacitive divider and controlled power flow conditioner for tapping electric power from the transmission line to rural distribution loads. References [12, 13] studied a method of electric field energy harvesting based on the principle of capacitance. Other papers [14–16] explored the feasibility of obtaining power from the shield wires of a transmission line. They indicated that this form of power supply can be a feasible and cost-effective alternative for feeding small loads existing along a high-voltage transmission line compared to other forms of power supply. Reference [17] presented a voltage stabilization system based on a step-down DC-DC converter for an energy acquisition system. Reference [18] proposed a new method of designing a low-cost substation to tap power from extrahigh voltage lines to power sparsely populated areas. Reference [19] investigated the equivalent circuit parameters of typical transmission lines at rated voltages from 110 kV to 1000 kV. References [20–22] researched the energy harvesting system of wireless sensors to realize the self-power of these nodes. Reference [23] described the development of an electromagnetic induction power supply system that obtained stable power from overhead ground wires. Reference [24] reported a simulation study on a power conversion module for an energy acquisition system that used the ground wire of the transmission line. Reference [25] used an overhead ground wire-based energy acquisition system to power a monitoring device for external breakage of transmission lines. Reference [26] analyzed and calculated the induced voltage and induced current on the insulated ground wire of an overhead transmission line and simulated the power acquired from the ground wire.

However, none of the above studies addressed the selection of a ground wire or the installation scheme of a ground wire-based energy acquisition system, and all ignored the influence of tower size on the power of the energy acquisition system. References [27, 28] studied the use of electromagnetic induction energy acquisition technology on the ground wires of typical overhead transmission lines, proposed energy acquisition schemes on the OPGW (Optical Fiber Composite Overhead Ground Wire), and on segmented insulated ground wires, respectively, and proposed an energy equivalent calculation circuit. References [29, 30] analyzed the power distribution characteristics of each energy acquisition point when multiple points were simultaneously energized on a typical overhead ground line. Reference [31] compared energy acquisition schemes between the OPGW and a segmented insulated ground wire on a typical overhead transmission line. These studies only analyzed energy acquisition schemes for a typical overhead ground wire with one OPGW and one segmented insulated ground wire. In practice, it is very common that both ground wires are segmented insulated ground wires. However, there has not been any literature report on the selection of energy acquisition schemes under this kind of ground wire configuration.

This study assumes that the key to the feasibility of ground wire energy acquisition lies in the adequacy of the power acquired. In this paper, the energy acquisition scheme and the parameter selection for an energy acquisition system for double-insulated ground wire were studied. Three energy acquisition schemes were proposed, and their equivalent circuit analysis models were established. The maximum power of the energy acquisition system was theoretically analyzed. The energy acquisition power of the three energy acquisition schemes for different tower-type sizes was compared and analyzed. A simulation model of a double-insulated ground wire energy acquisition system was built in PSCAD, and a simulation analysis was carried out. The effects of load impedance, length of energy acquisition wire, grounding resistance, and load current on the power acquired and the energy acquisition scheme were analyzed.

2. Energy Acquisition Method for Double-Segmented Insulated Ground Wires

The alternating current in the transmission line conductor generates an alternating electromagnetic field in space, and the ground wire in the alternating electromagnetic field generates an induced electromotive force. Induced current can be formed on the ground wire when the ground wire forms a closed loop with the earth or another ground wire. There is also a coupling capacitor between the ground wire and the conductor, and an electrostatic induction voltage can be generated on the ground wire. Because the ground wire is grounded, the electrostatic induction voltage is 0. Therefore, the electrostatic induction effect can be ignored.

Figure 1 shows an equivalent circuit diagram of the two ground wires of an overhead transmission line, both of which are segmented insulated ground wires. The two segmented insulated ground wires are SW1 and SW2, respectively. R_1, R_2, R_3, and R_4 represent the grounding resistances of the towers. SW1 and SW2 are directly grounded through R_2 and connected to other towers through lightning insulators. E_1, E_2, Z_{10}, and Z_{20} are the induced electromotive force and the equivalent impedance of SW1 and SW2, respectively. R represents the equivalent load resistance of the energy acquisition device.

The formulae for calculating the induced electromotive force on the ground wire are

$$\begin{aligned} \dot{E}_1 &= l \cdot 0.1445\left(\dot{I}_a \lg d_{a1} + \dot{I}_b \lg d_{b1} + \dot{I}_c \lg d_{c1}\right), \\ \dot{E}_2 &= l \cdot 0.1445\left(\dot{I}_a \lg d_{a2} + \dot{I}_b \lg d_{b2} + \dot{I}_c \lg d_{c2}\right), \end{aligned} \tag{1}$$

where l is the length of the ground wire (km); I_a, I_b, and I_c are the three-phase current transmitted by the conductor (A); and d_{a1}, d_{b1}, and d_{c1}, respectively, indicate the distances between the three conductors A, B, and C to the ground wire SW1 (m). In the case of a symmetrical arrangement, $d_{a1} = d_{c2}$, $d_{b1} = d_{b2}$, and $d_{c1} = d_{a2}$.

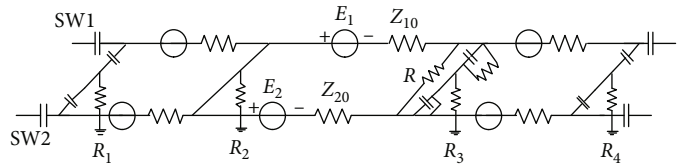

Figure 1: Equivalent circuit diagram of a double-segmented insulated ground wire.

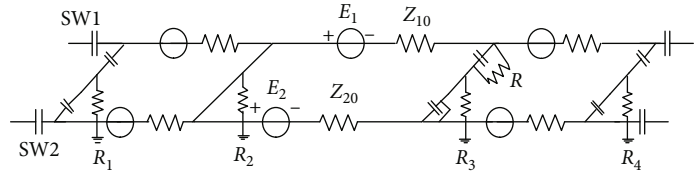

Figure 2: Schematic diagram of energy acquisition scheme I.

The equivalent impedance of the ground wire can be calculated as

$$Z_{10} = l\left(R_1 + 0.05 + j0.1445 \lg 660\sqrt{\rho/f}/r_1\right), \quad (2)$$

where R_1 is the resistance per unit length of ground wire SW1 (Ω/km); f is the frequency of the current (Hz); ρ is the soil resistivity (Ω·m); and r_1 is the effective radius of ground wire SW1 (m). Z_{20} is calculated in the same way as Z_{10}.

For a system where the two ground wires are both segmented insulated ground wires, there are three schemes for installing the energy acquisition device.

2.1. Energy Acquisition Scheme I. As shown in Figure 2, the high-potential end of the energy acquisition device is installed on the insulated ground wire, the low-potential end is installed on the iron tower, and the other ground wire is short-circuited with the discharge gap of the tower. In this scheme, the current circuit is composed of towers R_2 and R_3 and two ground wires SW1 and SW2, and its equivalent circuit is shown in Figure 3.

2.2. Energy Acquisition Scheme II. As shown in Figure 4, the two ends of the energy acquisition device are, respectively, installed on ground wire SW1 and the iron tower, and the gap between ground wire SW2 and the iron tower is not short-circuited. In this type of scheme, ground wire SW2 is not connected to the current loop, and the current loop is composed of ground wire SW1 and the ground. The equivalent circuit diagram is shown in Figure 5.

2.3. Energy Acquisition Scheme III. As shown in Figure 6, the two ends of the energy acquisition device are, respectively, installed on ground wire SW1 and ground wire SW2, and the gap between the ground line and the iron tower is not short-circuited. In this case, the current loop is composed of the two ground wires, and the equivalent circuit diagram is shown in Figure 7.

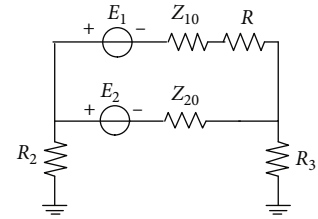

Figure 3: Equivalent circuit diagram of energy acquisition scheme I.

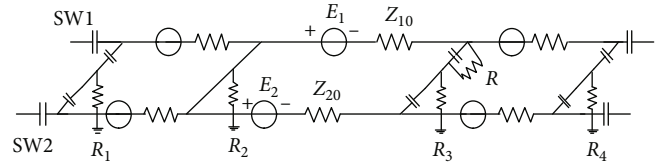

Figure 4: Schematic diagram of energy acquisition scheme II.

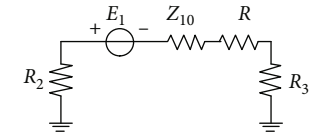

Figure 5: Equivalent circuit diagram of energy acquisition scheme II.

3. Equivalent Circuit Model and Power Analysis of Energy Acquisition Scheme

To perform a theoretical analysis of the power acquired by an energy acquisition device, a mathematical model of the energy acquisition circuit must be established. According to the equivalent circuit of each energy acquisition scheme described earlier, its mathematical model can be established using the Thevenin equivalence principle.

3.1. Energy Acquisition Scheme I. According to Figure 3, the power supply voltage u_{oc} and the internal impedance Z_{eq} of the equivalent circuit of energy acquisition scheme I are as follows:

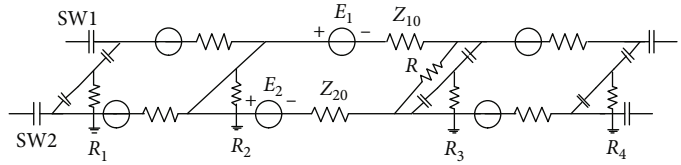

Figure 6: Schematic diagram of energy acquisition scheme III.

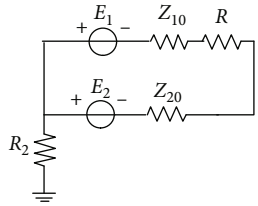

Figure 7: Equivalent circuit diagram of energy acquisition scheme III.

$$\begin{cases} u_{oc} = \dot{E}_2 - \dot{E}_1 - \dfrac{\dot{E}_2 \cdot Z_{20}}{Z_{20} + 2R}, \\ Z_{eq} = Z_{10} + \dfrac{Z_{20} \cdot 2R}{Z_{20} + 2R}, \end{cases} \tag{3}$$

where R is the tower grounding resistance.

The power acquired by the energy acquisition device is

$$P = \frac{u_{oc}^2 \cdot R_L}{\left(R_{eq} + R_L\right)^2 + \left(X_{eq} + X_L\right)^2}. \tag{4}$$

According to the impedance matching principle, when the load impedance Z_L of the energy acquisition device is conjugate with the internal impedance Z_{eq} of the equivalent circuit, the maximum power can be obtained, and the maximum active power is

$$P_{max} = \frac{u_{oc}^2}{4R_{eq}}. \tag{5}$$

3.2. Energy Acquisition Scheme II. According to Figure 5, the power supply voltage u_{oc} and the internal impedance Z_{eq} of the equivalent circuit of energy acquisition scheme II are as follows:

$$\begin{cases} u_{oc} = -\dot{E}_1, \\ Z_{eq} = Z_{10} + 2R. \end{cases} \tag{6}$$

The maximum acquisition power is derived, and the formula for the maximum power is as follows:

$$P_{max} = \frac{0.0052 \cdot l^2 I_a^2 \left[\left(\lg\left(d_{a1}/\sqrt{d_{b1}d_{c1}}\right)\right)^2 + 0.75(\lg\left(d_{b1}/d_{c1}\right))^2\right]}{l(R_1 + 0.05) + 2R}. \tag{7}$$

3.3. Energy Acquisition Scheme III. According to Figure 7, the power supply voltage u_{oc} and the internal impedance Z_{eq} of the equivalent circuit of energy acquisition scheme III are as follows:

$$\begin{cases} u_{oc} = \dot{E}_2 - \dot{E}_1, \\ Z_{eq} = Z_{10} + Z_{20}. \end{cases} \tag{8}$$

The maximum acquisition power is derived, and the formula for the maximum power of energy acquisition scheme III is as follows:

$$P_{max} = \frac{0.0078l \cdot I_a^2 \cdot \left(\lg\left(d_{c1}/d_{a1}\right)\right)^2}{R_1 + 0.05}. \tag{9}$$

4. Case Study

To obtain the maximum power from the energy acquisition device, this paper studies the influence of the spatial position relationship between the ground wire and the conductor, the load impedance, the length of energy acquisition wire, the grounding resistance, and the load current on the energy acquisition scheme.

4.1. Impact of Spatial Position Relationship between Ground Wire and Conductor. In different tower-structure types and sizes, the spatial relationship between the ground wire and the conductor is different, resulting in different induced voltages on the ground wire. By comparing the power of different energy acquisition schemes under different positional relationships between the ground wire and the conductor, a position space can be divided into four regions, as shown in Figure 8. The colors in Figure 8 are only used to distinguish different spatial regions and have no other meaning. The spatial position of the ground wire and the conductor has great influence on the power of the ground wire energy acquisition device. Different spatial relationships between ground wire and conductor lead to different optimal schemes for ground wire energy acquisition. In the region shown in Figure 8(a), scheme III is superior to scheme I, and scheme I is superior to scheme II. In the region shown in Figure 8(b), scheme II is superior to scheme I, and scheme I is superior to scheme III. In the region shown in Figure 8(c), scheme I is superior

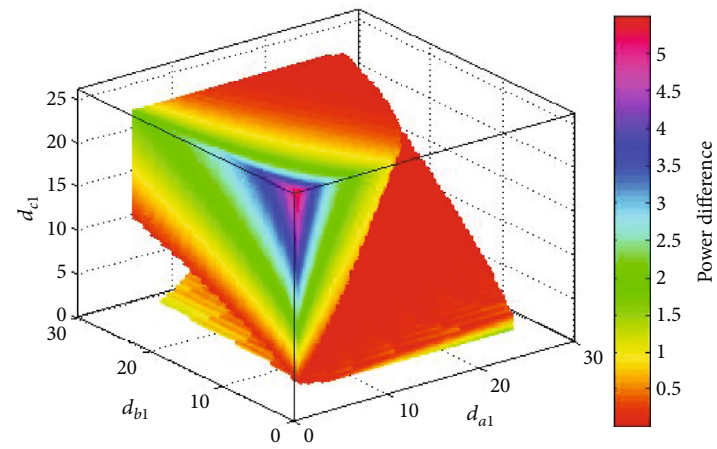

(a)

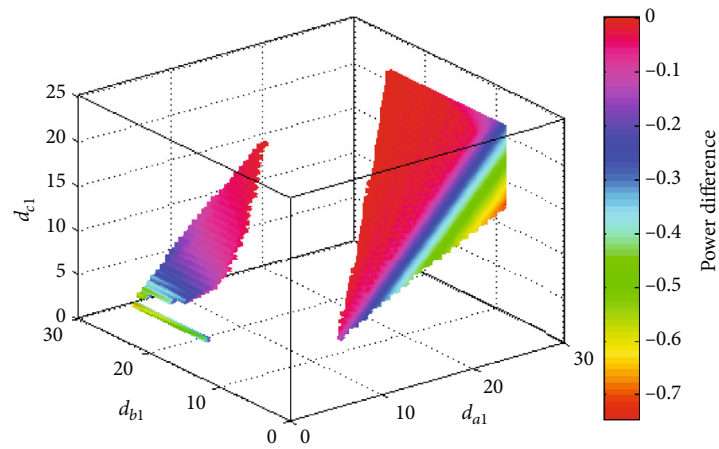

(b)

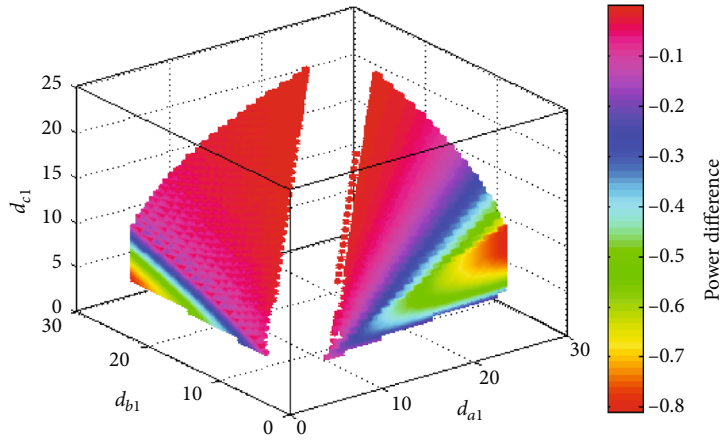

(c)

Figure 8: Continued.

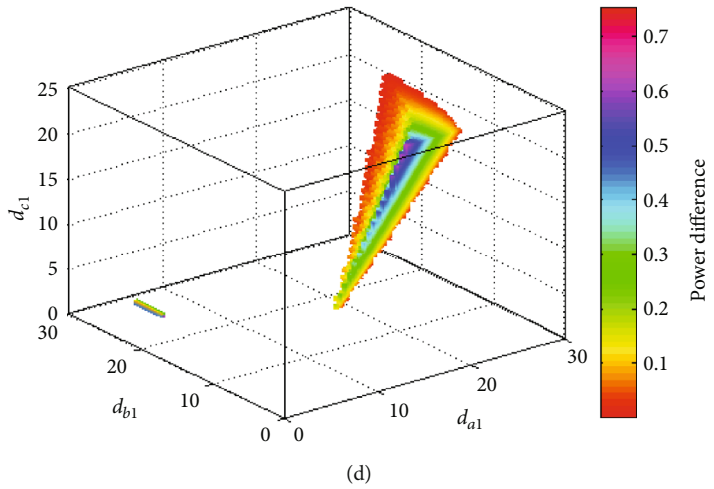

(d)

Figure 8: Spatial position relationship between ground wire and conductor and the power acquired.

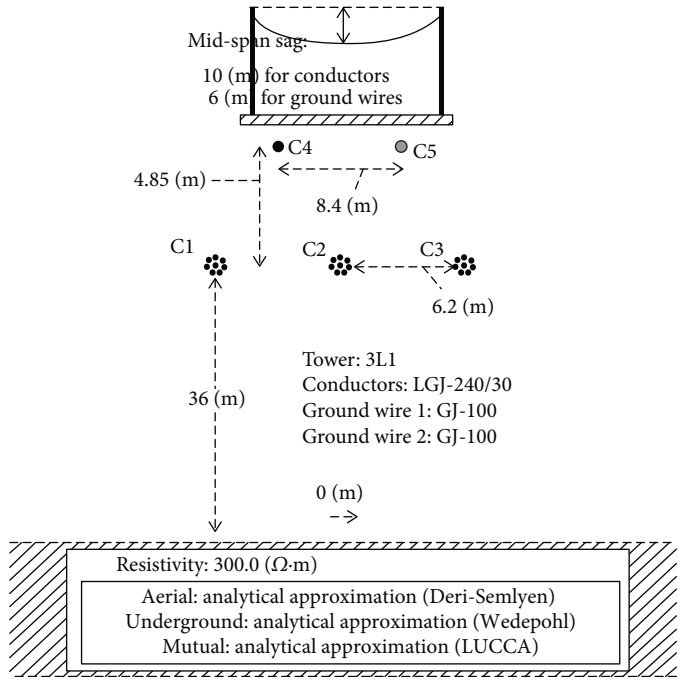

Figure 9: Simulation model of transmission line.

to scheme III, and scheme III is superior to scheme II. In the region shown in Figure 8(d), scheme II is superior to scheme III, and scheme III is superior to scheme I. The above results show that the optimal energy acquisition scheme and parameters for different transmission lines may be different. Therefore, in practical applications, each transmission line needs to be analyzed separately to design the optimal energy acquisition scheme and parameters.

To study the influence of load impedance, length of energy acquisition wire, grounding resistance, and load current on the energy acquisition scheme, four kinds of tower with different head size were selected in this study, with the spatial positions of ground wire and conductor belonging to the four regions in Figure 8, respectively.

Case 1. $d_{a1} = 5.2$ m, $d_{b1} = 6.4$ m, $d_{c1} = 11.5$ m. Their spatial positional relationship belongs to Figure 8(a).

Case 2. $d_{a1} = 23$ m, $d_{b1} = 7$ m, $d_{c1} = 18.5$ m. Their spatial positional relationship belongs to Figure 8(b).

Case 3. $d_{a1} = 9$ m, $d_{b1} = 19$ m, $d_{c1} = 11$ m. Their spatial positional relationship belongs to Figure 8(c).

Case 4. $d_{a1} = 14$ m, $d_{b1} = 5$ m, $d_{c1} = 18.5$ m. Their spatial positional relationship belongs to Figure 8(d).

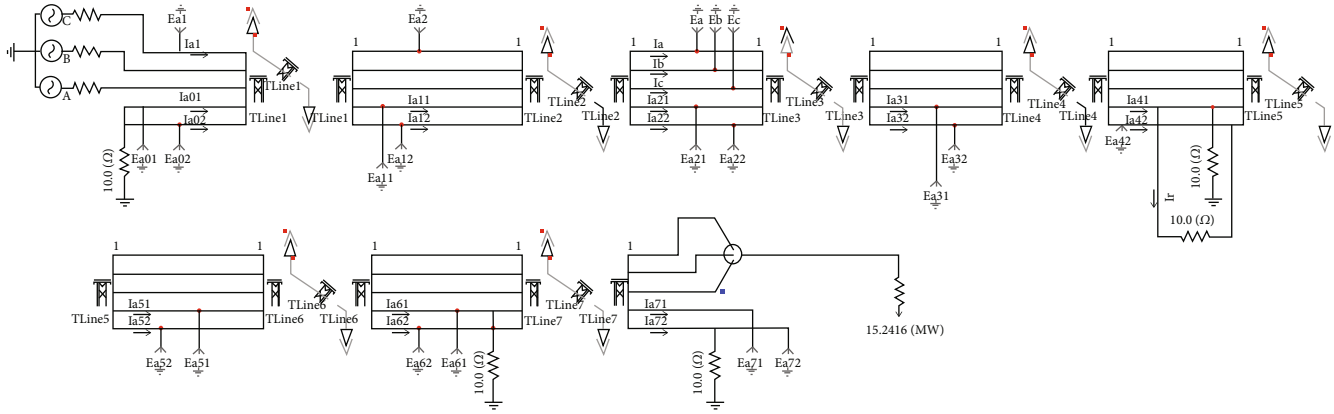

Figure 10: Simulation model of ground wire energy acquisition.

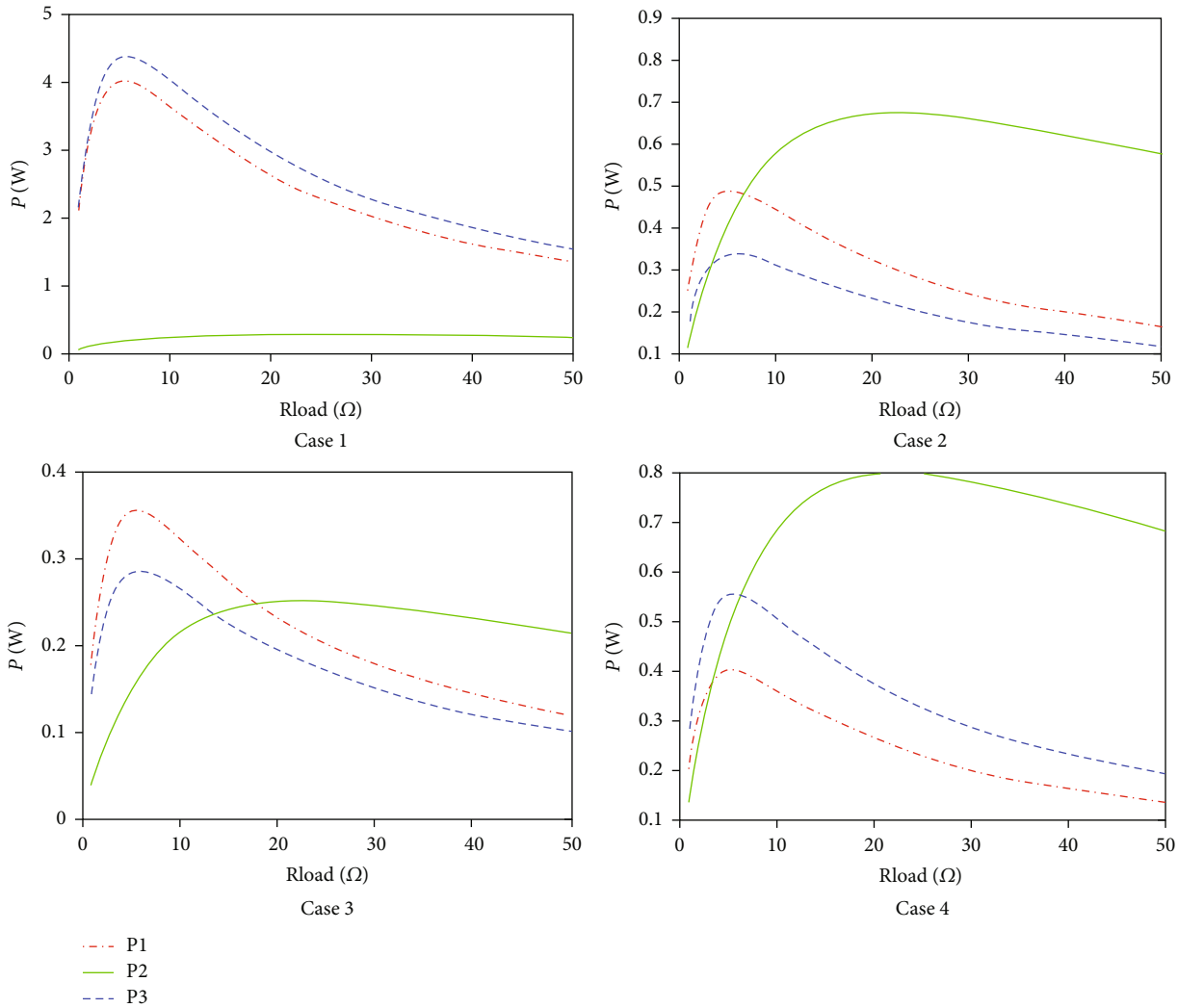

Figure 11: Variation of power with load impedances in different cases.

The voltage level of the transmission line is 110 kV. The two ground wires are segmented insulated ground wires with the same parameters. The resistance per unit length of ground wire R_1 is 1.16 Ω/km. The current frequency f is 50 Hz. The soil resistivity ρ is 300 Ω·m. The effective radius r_1 of the ground wire is 0.0065 m. The length of the energy acquisition wire l is 2 km. The tower grounding resistance R is 10 Ω. The load resistance of the energy acquisition device is 10 Ω. The load current of the transmission line is 80 A. In order to calculate the power acquired in the above cases, a

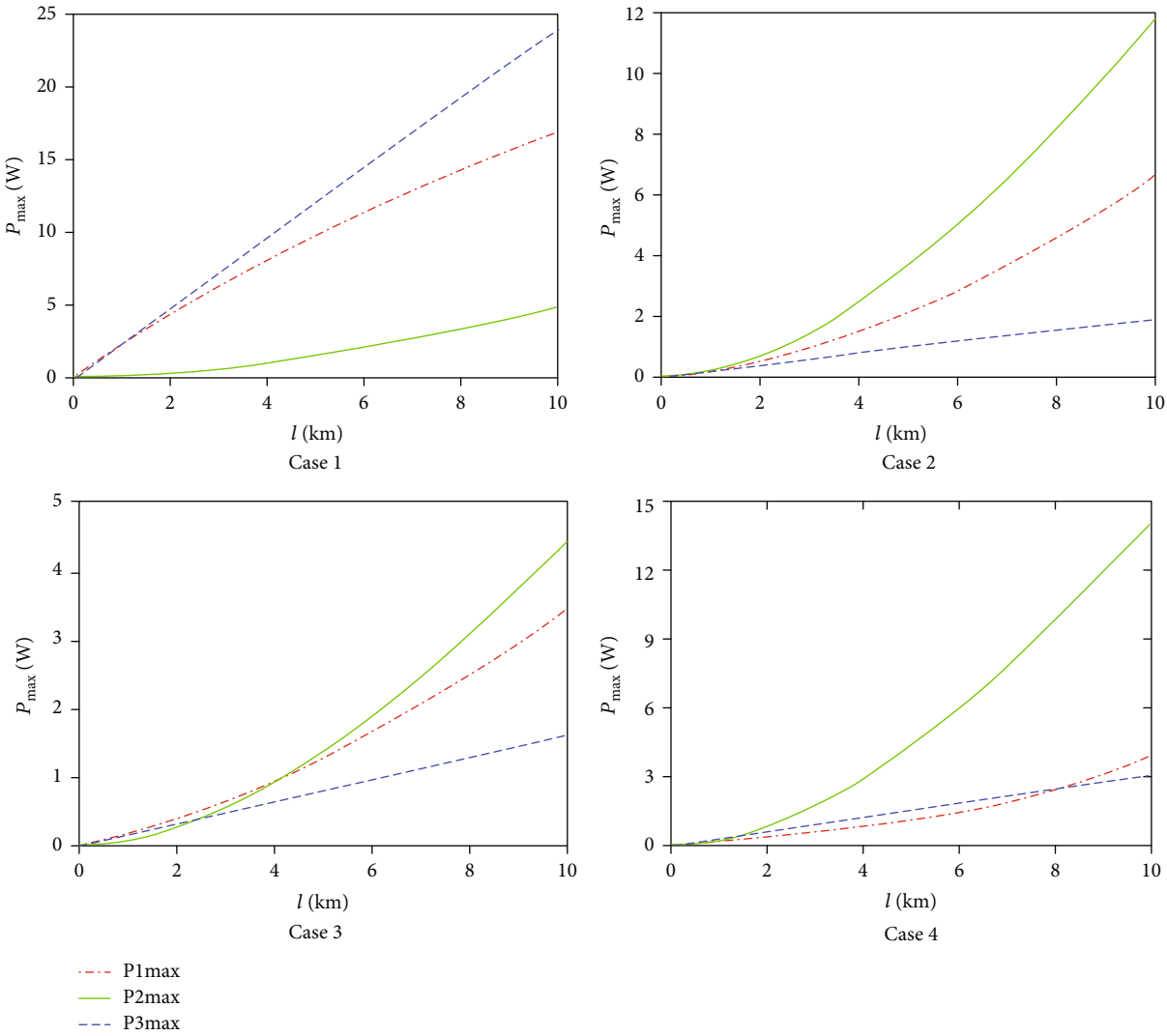

Figure 12: Variation of power with length of energy acquisition wire in different cases.

simulation model of ground wire energy acquisition was established in PSCAD. And the frequency-dependent phase model was used for the transmission line modeling, as shown in Figure 9. Figure 10 is a simulation diagram of scheme I, and the structure diagrams of scheme II and scheme III are similar.

4.2. Impact of Load Impedance. To study the influence of different load impedances on the electric power acquired under different schemes, it is assumed that the load impedance of the energy acquisition device varies between 1 and 50 Ω and that the power curve under each energy acquisition scheme is as shown in Figure 11. This figure shows that when the load impedance is less than the internal impedance of the equivalent power source, the electric power increases with increasing load impedance; when the load impedance is greater than the internal impedance of the equivalent power source, the electric power decreases with increasing load impedance; and when the load impedance is equal to the internal impedance of the equivalent power source, that is, when the impedance matches, the electric power reaches the maximum.

The equivalent power supply internal resistances of scheme I and scheme III are small, but the equivalent power supply internal resistance of scheme II is larger. In different tower types, the load impedance has different effects on the choice of energy acquisition scheme. For example, in Case 3, when the load impedance is less than 14 Ω, scheme I is superior to scheme III, and scheme III is superior to scheme II. When the load impedance is between 14 and 17 Ω, scheme I is superior to scheme II, and scheme II is superior to scheme III. When the load impedance is greater than 17 Ω, scheme II is superior to scheme I, and scheme I is superior to scheme III.

4.3. Impact of the Length of the Energy Acquisition Wire. For the case where the two ground wires are insulated ground wires, the power of the energy acquisition device is independent of the span between the two towers and is only related to the length of the wires between the grounding point and the

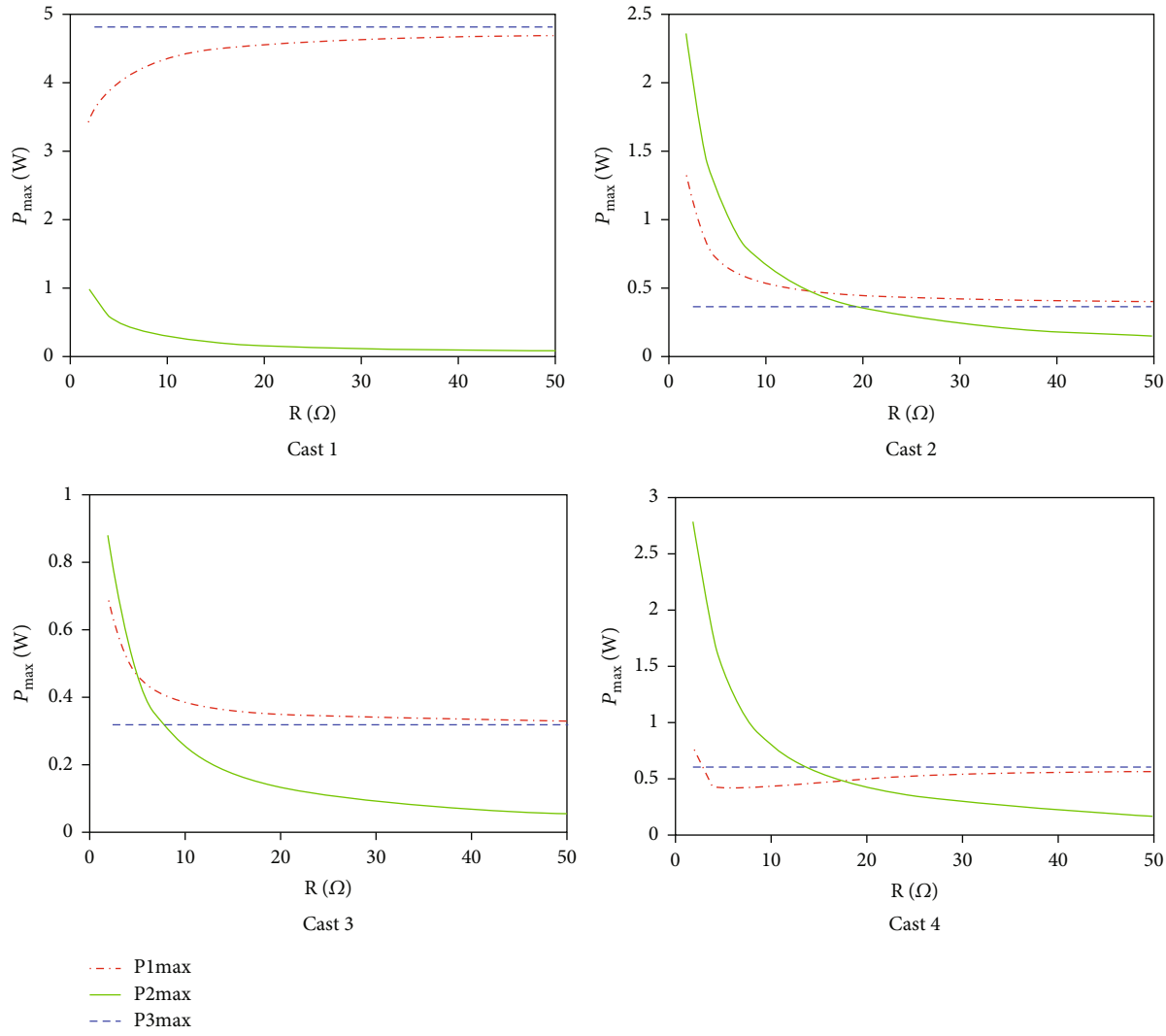

Figure 13: Variation of power with grounding resistance of the tower in different cases.

power collection point (i.e., the length of the energy acquisition wire). Assuming that the length of the energy acquisition wire varies between 0.1 and 10 km, the maximum power curve for each energy acquisition scheme is as shown in Figure 12. This figure shows that as the length of the energy acquisition wire increases, the maximum power increases, and the speed of increase is related to tower size.

In different tower types, the length of the energy acquisition wire has different effects on the choice of energy acquisition scheme. For example, in Case 3, when the length of the energy acquisition wire is less than 2.5 km, scheme I is superior to scheme III, and scheme III is superior to scheme II. When the length of the energy acquisition wire is between 2.5 and 4 km, scheme I is superior to scheme II, and scheme II is superior to scheme III. When the length of the energy acquisition wire is greater than 4 km, scheme II is superior to scheme I, and scheme I is superior to scheme III.

4.4. Impact of the Grounding Resistance of the Tower. To study the influence of the grounding resistance of the tower on the maximum power acquired by the energy acquisition device, it is assumed that the grounding resistance varies between 2 and 50 Ω. Figure 13 shows the maximum power curve under each energy acquisition scheme. It is clear that the maximum power of scheme III is not affected by the grounding resistance, but that the maximum power of scheme II decreases with increasing grounding resistance. However, the maximum power variation of scheme I is complex. In Case 1, the maximum power of scheme I increases with increasing the grounding resistance. In cases 2 and 3, the maximum power of scheme I decreases with increasing grounding resistance. When the grounding resistance is greater than 15 Ω, its influence on power tends to be stable. In Case 4, the power of scheme I is no longer monotonic. When the grounding resistance is less than 5 Ω, the power of scheme I decreases with increasing grounding resistance, but when the grounding resistance is greater than 5 Ω, the power of scheme I increases with increasing grounding resistance.

The grounding resistance of the tower has an influence on the choice of energy acquisition scheme. Because the influence of grounding resistance on each energy acquisition scheme is different, the optimal energy acquisition scheme

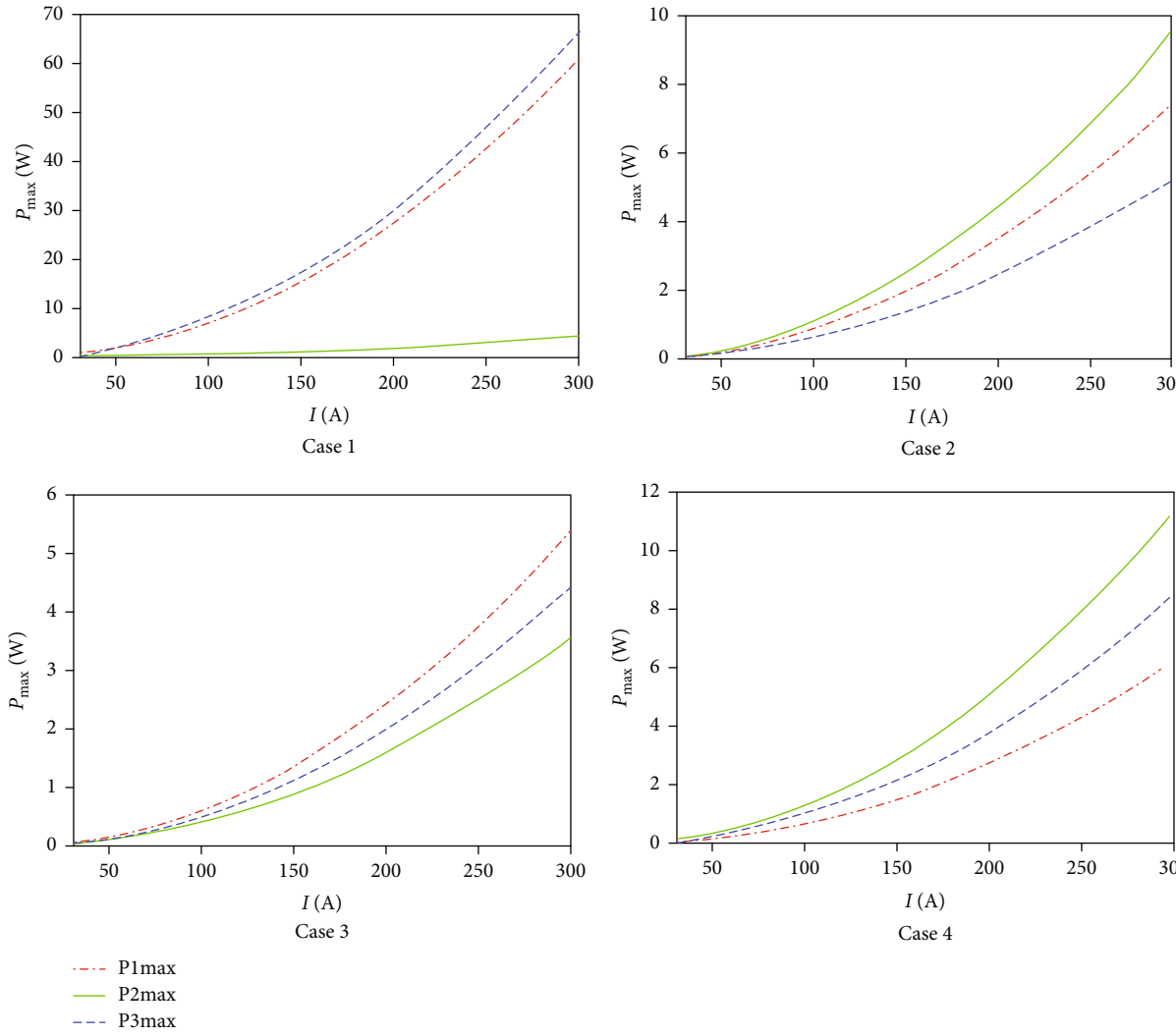

Figure 14: Variation of power with load current in different cases.

under different grounding resistances is different. For example, in Case 3, when the grounding resistance is less than 5 Ω, scheme II is superior to scheme I, and scheme I is superior to scheme III. When the grounding resistance is between 5 and 7 Ω, scheme I is superior to scheme II, and scheme II is superior to scheme III. When the grounding resistance is greater than 7 Ω, scheme I is superior to scheme III, and scheme III is superior to scheme II.

4.5. Impact of Load Current. To study the influence of transmission line current on the maximum power of the energy acquisition device, it is assumed that the load current varies between 30 and 300 A. The maximum power curve under each energy acquisition scheme is shown in Figure 14. This figure shows that the maximum power of the three energy acquisition schemes increases with increasing load current and that the choice of energy acquisition scheme is not affected by the magnitude of the load current.

4.6. Selection of Energy Acquisition Scheme and Parameters. According to the above analysis, the energy acquisition scheme for a double-insulated ground wire is affected by the spatial positional relationship between the ground wire and the conductor, the load impedance, the length of the energy acquisition wire, and the grounding resistance of the tower. Therefore, in practical application, according to these relationships, it is necessary to consider comprehensively the impedance of the energy acquisition system and the length of the energy acquisition wire and on this basis to select the installation scheme for the energy acquisition device.

In practical application, for a transmission line that has already been put into operation, its tower type, distance between wires, and operating parameters have been determined. Therefore, when designing an energy acquisition device, it is only necessary to consider the load impedance, the length of the energy acquisition wire, and the grounding resistance of the tower to select the energy acquisition scheme and parameters. They can be determined in turn according to the following steps.

First, select the length of the energy acquisition ground wire according to the required power and the curve of the power with the length of the energy acquisition wire. Assume

Table 1: The main parameters of the energy acquisition system.

Key parameters	Value
Spatial position relationship between ground wire and conductors	$d_{a1} = d_{c2} = 5.2$ m, $d_{b1} = d_{b2} = 6.4$ m, and $d_{c1} = d_{a2} = 11.5$ m
Average load current of the transmission line	80 A
Length of the energy acquisition ground wire	1.187 km
Grounding resistance of tower whose ground wire shorted	9.4 Ω
Load resistance of the energy acquisition device	8.6 Ω
Designed power	2.08 W

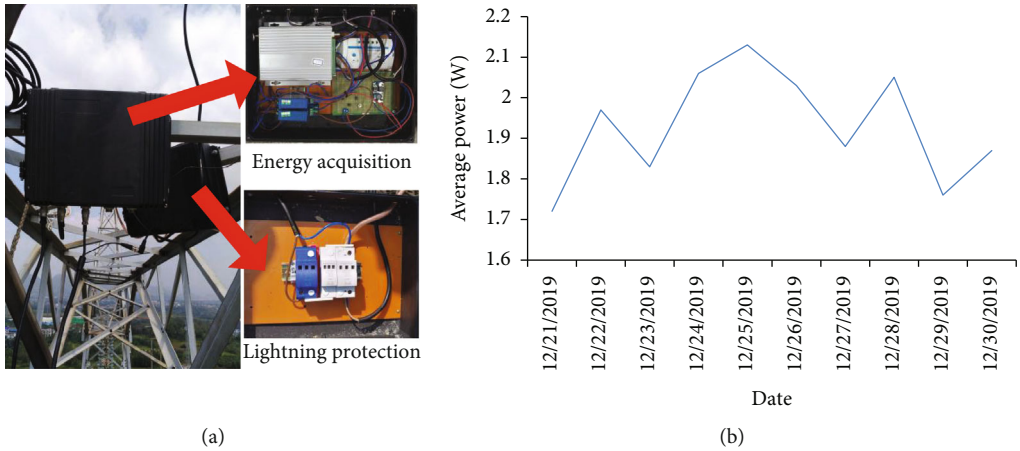

Figure 15: The field-installed energy acquisition device and its daily average power acquired.

that in Case 3, the load requires the maximum power of the energy acquisition device to be not less than 2 W, as shown in Figure 12, scheme II is optimal, and the length of the energy acquisition ground wire should not be less than 6 km.

Secondly, according to the grounding resistance of each tower and the variation curve of the power with the grounding resistance of the tower, select another tower in the energy acquisition loop. It can be known from Figure 13 that, within the adjacent range of not less than 6 km of the energy acquisition ground wire length, select a tower with the grounding resistance less than 10 Ω as the tower with its ground wire shorted.

Finally, according to the variation curve of the power with the load impedance, the optimal load impedance of the energy acquisition device is selected. It can be known from Figure 11 that in scheme II, the optimal impedance value of the energy acquisition device is 20 Ω, and then the impedance conversion circuit is designed according to the actual impedance value of the load to achieve impedance matching.

A designed energy acquisition device was installed and operated on the actual transmission line. The main parameters of the energy acquisition system were shown in Table 1. The value of other parameters was the same as those in Section 4.1. The installation method of the device was scheme III. Based on the above parameters, the theoretical analysis has shown that the power acquired by the device was 2.08 W. The field-installed energy acquisition device was shown in Figure 15(a). It consisted of an energy acquisition box and a lightning protection box. Its daily average power acquired from December 21 to December 30 was shown in Figure 15(b). Its power fluctuation was mainly affected by the load current. As can be seen in Figure 15(b), the average power acquired for 10 days was 1.93 W, which was close to the theoretical design value. The difference between the actual acquired power and the designed value is mainly affected by the load current fluctuation. The power acquired basically meets the design requirements, which shows that the method proposed in this paper is effective.

5. Conclusions

In this study, an energy acquisition scheme and its parameter selection in the case of double-insulated ground wire have been considered. According to the characteristics of double-insulated ground wire, three energy acquisition schemes have been proposed, and equivalent circuit analysis models for the three schemes have been developed. The maximum power acquired by the three energy acquisition schemes has also been analyzed. The power acquired by the three energy acquisition schemes under different tower sizes has been compared and analyzed. The research results show that the relative spatial position of the ground wire and the conductor has a great influence on the power acquisition of the ground wire. Different spatial relationships between ground wires and conductors can change the optimal scheme for energy acquisition.

A simulation model of the double-insulated ground wire-based energy acquisition system was built in PSCAD, and a

simulation analysis was carried out. The effects of load impedance, length of energy acquisition wire, grounding resistance, and load current on the power acquired were analyzed. The conclusions obtained are as follows:

(i) When the load impedance is equal to the internal impedance of the equivalent power source, the power of the energy acquisition system reaches the maximum

(ii) As the length of the energy acquisition wire increases, the maximum power increases, and the speed of increase is related to tower size

(iii) The maximum power of scheme III is not affected by grounding resistance, and the maximum power of scheme II decreases with increasing grounding resistance. However, the maximum power variation of scheme I is complex and is related to tower size

(iv) The maximum power of the three energy acquisition schemes increases with increasing load current, and the choice of energy acquisition scheme is not affected by the magnitude of the load current

(v) In different tower types, the load impedance, length of energy acquisition wire, and grounding resistance have different effects on the choice of energy acquisition scheme. In practical applications, it is necessary to consider comprehensively the factors described above to select the energy acquisition scheme and its parameters

Data Availability

The data used to support the findings of this study are included within the article.

Conflicts of Interest

The authors declare that there is no conflict of interest regarding the publication of this paper.

Acknowledgments

This research was funded by the science and technology project of State Grid Hunan Electric Power Company Limited (grand number: 5216AF18000A).

References

[1] R. Horton, M. Halpin, and K. Wallace, "Induced voltage in parallel transmission lines caused by electric field induction„" in *ESMO 2006 - 2006 IEEE 11th International Conference on Transmission & Distribution Construction, Operation and Live-Line Maintenance*, pp. 1–7, Albuquerque, NM., 2006.

[2] C. D. Xue, X. H. Yang, D. X. Cui, and J. Jiang, "Test and analysis of inductive voltage on overhead ground wire of 1000 kV UHV AC line," *High Voltage Engineering*, vol. 35, no. 8, pp. 1802–1806, 2009.

[3] C. Li, *Research of Electricity Extraction Technology Based on the Transmission Lines*, North China Electric Power University, Beijing, 2013.

[4] X. Lu, J. Yang, S. Fan, Z. Liu, and K. Zhang, "An on-line energy acquisition method for transmission lines based on impedance matching," *Journal of Electric Power*, vol. 34, 2019.

[5] Z. Liu, S. Fan, and J. Hu, "Research on on-line energy acquisition method for transmission lines based on impedance matching," *Proceedings of the CSEE*, vol. 8, no. 23, pp. 1–12, 2019.

[6] X. Li, L. Du, W. Chen, Y. Wang, C. Sun, and J. Li, "A novel scheme of draw-out power supply utilized in transmission line state monitoring," *Automation of Electric Power Systems*, vol. 1, pp. 76–80, 2008.

[7] L. Xiong, Y. Z. He, D. J. Song, Y. Liu, W. He, and Z. L. Zhang, "Design on power supply for the transmission line on-line monitoring equipment," *High Voltage Engineering*, vol. 36, no. 9, pp. 2252–2257, 2010.

[8] M. Aredes, C. Portela, and F. C. Machado, "A 25-MW soft-switching HVDC tap for ±500-kV transmission lines," *IEEE Transactions on Power Delivery*, vol. 19, no. 4, pp. 1835–1842, 2004.

[9] W. Wang, X. Huang, L. Tan, J. Guo, and H. Liu, "Optimization design of an inductive energy harvesting device for wireless power supply system overhead high-voltage power lines," *Energies*, vol. 9, no. 4, p. 242, 2016.

[10] A. Costanzo, M. Dionigi, D. Masotti et al., "Electromagnetic energy harvesting and wireless power transmission: a unified approach," *Proceedings of the IEEE*, vol. 102, no. 11, pp. 1692–1711, 2014.

[11] A. A. Jimoh, J. Munda, A. C. Britten, and D. V. Nicolae, "Controlled power flow capacitive divider for electric power tapping," *Acta Press Anaheim, PO BOX*, vol. 2481, pp. 113–118, 2006.

[12] D. Zhao, L. Li, and D. Dai, "Electric field energy harvesting for on-line condition-monitoring device installed on high-voltage transmission tower," *Electronics Letters*, vol. 51, no. 21, pp. 1692-1693, 2015.

[13] M. J. Moser, T. Bretterklieber, H. Zangl, and G. Brasseur, "Strong and weak electric field interfering: capacitive icing detection and capacitive energy harvesting on a 220-kV high-voltage overhead power line," *IEEE Transactions on Industrial Electronics*, vol. 58, no. 7, pp. 2597–2604, 2011.

[14] R. L. Vasquez-Arnez, M. Masuda, J. A. Jardini, and E. J. V. Nicodem, "Tap-off power from a transmission line shield wires to feed small loads," in *2010 IEEE/PES Transmission and Distribution Conference and Exposition: Latin America (T&D-LA)*, pp. 116–121, Sao Paulo, 2010.

[15] R. L. Vasquez-Arnez, M. Masuda, J. A. Jardini, W. Kaiser, and E. J. V. Nicodem, "Tap-off power from the overhead shield wires of an HV transmission line," *IEEE Transactions on Power Delivery*, vol. 27, no. 2, pp. 986–992, 2012.

[16] Y. S. Aswani and S. Hassainar, "Regulation of the extracted energy induced in shield wires of an HV transmission line," *International Journal of Engineering Research & Technology*, vol. V4, no. 4, pp. 1332–1336, 2015.

[17] R. L. Vasquez-Arnez, M. Masuda, J. A. Jardini, and E. J. V. Nicodem, "Tap-off power from overhead ground wires: its feasibility and voltage stabilization system," in *2011 IEEE Trondheim PowerTech*, pp. 1–7, Trondheim, 2011.

[18] R. Lategan, *Design Guide for Power Tapping from Extra-High Voltage (EHV) Lines Using Insulated Shield-Wire and Series*

Compensation, with Standardised Components, Bloemfontein, Central University of Technology, 1998.

[19] G. Qi, Y. Zheng, K. Xia, W. Wu, F. Liao, and S. Shu, "Equivalent circuit parameters of power tap-off from insulated shield wires of high voltage transmission lines at different rated voltages," in *2018 IEEE International Conference on High Voltage Engineering and Application (ICHVE)*, pp. 1–4, Athens, Greece, 2018.

[20] X.-F. Zhang and C.-C. Yin, "Energy harvesting and information transmission protocol in sensors networks," *Journal of Sensors*, vol. 2016, Article ID 9364716, 5 pages, 2016.

[21] F. Guo, H. Hayat, and J. Wang, "Energy harvesting devices for high voltage transmission line monitoring," in *2011 IEEE Power and Energy Society General Meeting*, pp. 1–8, Detroit, MI, USA, 2011.

[22] S. Ahmed, Y. D. Lee, S. H. Hyun, and I. Koo, "A cognitive radio-based energy-efficient system for power transmission line monitoring in smart grids," *Journal of Sensors*, vol. 2017, 12 pages, 2017.

[23] T. Yamaguchi, S. Takano, O. Naganuma, M. Matsuoka, H. Nakamura, and K. Tomonaga, "Development of power supply system for obstruction lights exploiting induced current which flows through overhead ground wires," in *EEE/PES Transmission and Distribution Conference and Exhibition*, pp. 2176–2180, Yokohama, Japan, 2002.

[24] L. Ding, G. Li, W. Li et al., "Simulation of source transformation module for electricity generating system based on overhead ground wires in the high-voltage power lines," *Chinese Journal of Electron Devices*, vol. 41, no. ss6, pp. 1422–1425, 2018.

[25] S. Huang and B. Xu, "Research and application of overhead ground wire acquisition and microwave detection in fault diagnosis of transmission line," *Electrical Engineering*, vol. 19, no. 10, pp. 6–9, 2018.

[26] Y. Li, *Research on the Energy Extracting Technology for Insulation Ground Wire of High Voltage Transmission Line*, North China Electric Power University, Beijing, 2016.

[27] X. I. Yanbin, J. I. Xingliang, H. Jianlin, Z. Zhijin, F. Songhai, and F. Caijin, "Study on power-tapping from segmented insulation ground wire of typical overhead transmission line," *Proceedings of the CSEE*, vol. 38, no. 3, pp. 947–955, 2018.

[28] J. I. Xingliang, X. I. Yanbin, and H. U. Jianlin, "Analysis of equivalent circuit for tapping electromagnetic power from overhead ground wires of typical transmission lines," *Power System Technology*, vol. 39, no. 7, pp. 2052–2057, 2015.

[29] Y. Xie, J. Tang, L. Lin, W. Yi, Z. Peng, and Y. Wen, "Power distribution characteristics of multi-point energy acquisition for overhead transmission lines," *Journal of Shaoyang University*, vol. 15, no. 4, pp. 54–61, 2018.

[30] Y. Xie, X. Wang, Q. Luo, and J. Liu, "Power distribution feature of coil-based power-tapping from ground wire of typical HV overhead transmission line," in *Proceedings of the 3rd International Conference on Advances in Energy and Environmental Science 2015*, pp. 1158–1162, Zhuhai, China, 2015.

[31] Y. Liu, Z. Xue, Y. Gong, X. Jiang, Y. Xie, and J. Hu, "Selection of electromagnetic energy acquisition ground wire for typical overhead transmission lines," *Sichuan Electric Power Technology*, vol. 38, no. 5, 2015.